

BOOTSTRAP ALGEBRAIC MULTIGRID FOR THE 2D WILSON DIRAC SYSTEM

J. BRANNICK[‡] AND K. KAHL[§]

Key words. QCD, Wilson discretization, bootstrap AMG, Kaczmarz relaxation, odd-even reduction, multigrid eigensolver.

AMS subject classification. 65F10, 65N55, 65F30

Abstract. We develop an algebraic multigrid method for solving the non-Hermitian Wilson discretization of the 2-dimensional Dirac equation. The proposed approach uses a bootstrap setup algorithm based on a multigrid eigensolver. It computes test vectors which define the least squares interpolation operators by working mainly on coarse grids, leading to an efficient and integrated self learning process for defining algebraic multigrid interpolation. The algorithm is motivated by the γ_5 -symmetry of the Dirac equation, which carries over to the Wilson discretization. This discrete γ_5 -symmetry is used to reduce a general Petrov Galerkin bootstrap setup algorithm to a Galerkin method for the Hermitian and indefinite formulation of the Wilson matrix. Kaczmarz relaxation is used as the multigrid smoothing scheme in both the setup and solve phases of the resulting Galerkin algorithm. The overall method is applied to the odd-even reduced Wilson matrix, which also fulfills the discrete γ_5 -symmetry. Extensive numerical results are presented to motivate the design and demonstrate the effectiveness of the proposed approach.

1. Introduction. Lattice quantum chromodynamics (QCD) is a numerical approach for computing observables of quarks, elementary particles, in cases where perturbative methods diverge, see [19] for an overview. Simulations of quarks require approximating the QCD path integral using Monte Carlo methods, which involves generating discrete realizations of the gauge fields and, then, computing observables by averaging over these ensembles of configurations. In both of these stages of a lattice QCD calculation, the discretized Dirac equation

$$D\psi = b \tag{1.1}$$

needs to be solved for numerous realizations of the gauge fields and, then, multiple right hand sides for each configuration. In this paper, we consider Wilson's discretization [36] of the Dirac equation so that $D = D_0 + mI$, where D_0 denotes the non-Hermitian mass-less Wilson matrix and the shift m is related to the mass of the quarks. We refer to D as simply the Wilson matrix implying that a particular shift m is associated with it.

All existing lattice QCD algorithms suffer from what is referred to as *critical slowing down*, which is a direct result of the structure of the Wilson matrix. Specifically, as the shift, m , approaches physically relevant values the minimal eigenvalues of D approach zero linearly, which leads to a highly ill-conditioned system of equations and the stalling convergence of standard Krylov subspace methods when applied to this system. As a result, the overall simulation becomes too costly at light masses and up until now this has led to the use of non-physical heavy quark masses in lattice

[‡]Department of Mathematics, Pennsylvania State University, University Park, PA 16802, USA (brannick@psu.edu). Brannick's work was supported by the National Science Foundation under grants OCI-0749202 and DMS-810982.

[§]Fachbereich Mathematik und Naturwissenschaften, Bergische Universität Wuppertal, D-42097 Wuppertal, Germany, (kkahl@math.uni-wuppertal.de). Kahl's work was supported by the Deutsche Forschungsgemeinschaft through the Collaborative Research Centre SFB-TR 55 "Hadron Physics from Lattice QCD"

QCD simulations. This, in turn, has motivated the extensive research that has been dedicated to the development of suitable multigrid preconditioners for discretizations of the Dirac equation over the past three decades, see [13, 14, 15, 16, 17, 18, 25].

The task of designing effective multigrid preconditioners for the Wilson matrix is further complicated by the fact that the near kernel modes, i.e., the vectors x such that $Dx \approx 0$ or $D^H x \approx 0$, are locally non-smooth. To be more precise, their entries depend significantly on the specific values of the given gauge field configuration, and, a precise understanding of this dependence is not well understood theoretically, yet. As a result, while earlier efforts in designing multigrid methods for discretizations of the Dirac equation did lead to marked improvements in some cases, methods with the potential to effectively remove critical slowing down in general have emerged only in the past few years in the context of adaptive [28] or bootstrap [6] algebraic multigrid (AMG).

The main new component of the adaptive and bootstrap AMG approaches is the idea to use the AMG hierarchy to expose prototype(s) of the near kernel (test vectors) that are not effectively treated by the solver and, then, adapt the coarse spaces to incorporate them. In *adaptive AMG* [11, 28], the solver is applied to appropriately formulated homogeneous problems on different grids to compute a single test vector, which is then used to update the restriction, interpolation, and coarse-grid operators on all grids. This gives a new solver which can be used in another adaptive cycle. The process is then repeated in a sequence of adaptive cycles until an efficient solver has been constructed. In contrast, *bootstrap AMG* uses relaxation and a multigrid (eigen)solver based on the emerging AMG hierarchy to compute a collection of test vectors in each of the bootstrap cycles and, then, a local least squares problem is formulated to define interpolation operators that approximate these vectors collectively.

Adaptive and bootstrap AMG setup algorithms have been developed for smoothed aggregation multigrid [28], element-free AMG [35], and classical AMG [6, 7, 10, 11]. Promising results of two- and three-grid adaptive aggregation AMG preconditioners for the Wilson and Wilson Clover discretizations of the Dirac equation are found in [2, 30] and in these works it has been demonstrated that adaptive AMG techniques can be used to construct effective preconditioners for the Wilson matrix. Some progress on combining adaptive AMG and bootstrap AMG techniques to develop preconditioners for the Wilson and Wilson Clover formulation has also been made [1, 7, 22]. These developments have shown that the bootstrap AMG approach, when combined with adaptive AMG, has the potential to dramatically reduce the costs of the adaptive setup process.

In this paper, we design and analyze a multigrid solver for the Wilson matrix based on the bootstrap AMG framework. The proposed approach builds on our work in [7], where we developed bootstrap AMG for solving Hermitian and positive definite linear systems of equations

$$Au = f.$$

Of particular interest in this previous work was the development of a bootstrap setup algorithm for the gauge Laplacian system with an emphasis on highly disordered gauge fields. Since the gauge Laplacian is Hermitian and positive definite, a Galerkin scheme based on a variational principle is the natural approach for solving this problem. The associated two-grid method involves a stationary linear iterative method (smoother) applied to the fine-grid system, and a coarse-grid correction: given an approximation $w \in \mathbb{C}^n$, compute an update $v \in \mathbb{C}^n$ by

1. Pre-smoothing: $y = w + M(f - Aw)$,
2. Correction: $v = y + PA_c^{-1}P^H(f - Ay)$, $A_c = P^HAP$.

Here, M is the approximate inverse of A that defines the smoother and $P : \mathbb{C}^{n_c} \mapsto \mathbb{C}^n$ with $n_c < n$ is the interpolation operator that maps information from the coarse to the fine grid. In the variational Galerkin scheme, restriction is defined by the conjugate transpose P^H of P . Thus the error propagation operator for a Galerkin two-grid method with one pre-smoothing step is given by

$$E_G = (I - PA_c^{-1}P^HA)(I - MA).$$

A multigrid algorithm is then obtained by recursively solving the coarse-grid error equation, involving A_c , using another two-grid method.

Generally, there are two AMG approaches for solving non-Hermitian problems like (1.1) involving the non-Hermitian Wilson matrix D , Galerkin [3, 5] and Petrov Galerkin [1, 12, 32] methods. A Petrov Galerkin method differs from the above Galerkin approach in that the restriction operator $R : \mathbb{C}^n \mapsto \mathbb{C}^{n_c}$ is no longer chosen as P^H . Consequently the coarse-grid operator is given by $D_c = RDP$. The error propagation operator of a Petrov Galerkin method applied to D , with one pre-smoothing step is then

$$E_{PG} = (I - PD_c^{-1}RD)(I - MD).$$

In [12], heuristic motivation and two-grid convergence theory of a Petrov Galerkin AMG approach in which the coarse spaces are constructed to approximate left and right singular vectors with small singular values are developed for non-Hermitian problems. The basic result that motivates this approach is as follows.

Let $\sigma_1 \leq \dots \leq \sigma_n$ be the singular values of the matrix D , i.e., $D = U\Sigma V^H$, with U and V unitary, and $\Sigma = \text{diag}(\sigma_1, \dots, \sigma_n)$, then it follows that $\sigma_1 \leq |\lambda| \leq \sigma_n$, for any eigenvalue λ of D . This suggests that the right and left near kernel vectors, i.e., x and y such that

$$\frac{\|Dx\|}{\|x\|} \approx \min_v \frac{\|Dv\|}{\|v\|} \quad \text{and} \quad \frac{\|D^Hy\|}{\|y\|} \approx \min_w \frac{\|D^Hw\|}{\|w\|},$$

are dominated by singular vectors rather than eigenvectors. To be more precise, let $W = VU^H$ and define the Hermitian positive definite matrices $WD = (D^HD)^{\frac{1}{2}}$ and $DW = (DD^H)^{\frac{1}{2}}$. Then the original non-Hermitian system $D\psi = b$ can be reformulated in two ways as an equivalent Hermitian system using WD or DW as the system matrix. Now, the fact that the eigenvectors corresponding to the minimal eigenvalues of WD are the right singular vectors corresponding to the minimal singular values of D and those for DW are the left singular vectors corresponding to minimal singular values of D and because WD and DW are Hermitian positive definite, they can be used to derive an approximation property for the original problem involving D , assuming that R is based on left singular vectors and P is based on right singular vectors corresponding to small singular values. Two grid convergence then follows from this approximation property together with the use of a suitable smoother.

We use this same reasoning to motivate the design of the proposed multigrid bootstrap AMG setup algorithm for the Wilson system. We begin by considering a general Petrov Galerkin bootstrap AMG setup strategy for computing left and right singular vectors of D , implicitly based on the equivalent Hermitian and indefinite formulation

of the singular value decomposition (SVD) [24, 27]. Then, we use the γ_5 -symmetry that the Dirac matrix satisfies to derive a relation between the subspaces spanned by left and right singular vectors with small singular values, as well as a relation between the right singular vectors of D and the eigenvectors of the Hermitian and indefinite form of the Wilson matrix $Z = \Gamma_5 D$, where Γ_5 is a simple unitary matrix. Finally, using these observations and a structure preserving form of interpolation we are able to reduce the general Petrov Galerkin approach to an equivalent Galerkin based coarsening scheme applied to Z . Further, because in our construction the resulting Galerkin coarse-grid operators also satisfy the γ_5 -symmetry on all grids, the equivalence of the proposed Petrov Galerkin setup process for D and the Galerkin scheme for Z also holds on all grids.

Since the Wilson discretization of the Dirac equation is formulated on a structured grid, we exploit this structure in the implementation of the proposed approach. Instead of solving systems with the Dirac matrix D we solve linear systems involving the Schur complement resulting from odd-even (red-black) reduction of the Wilson matrix D as considered in [2, 21]. We use a classical AMG [8, 9] form of interpolation with full coarsening (cf. Section 3.2) on all grids of the hierarchy. The non-zero entries of P are chosen based on the structure as well and interpolation weights are computed row-wise using a least squares interpolation approach [7]. The setup we use in the implementation of the proposed algorithm combines a bootstrap setup based on a multigrid eigensolver with adaptive AMG cycles. We mention that such a bootstrap-adaptive setup process has previously been considered in the context of developing eigensolvers for computing state vectors in Markov chain applications [4].

We chose to use Kaczmarz relaxation both in the setup and solve phases of the proposed algorithm, which gives a stationary smoother that is guaranteed to converge for the Wilson matrix. Using a convergent stationary smoother allows us to access and analyze the performance of the resulting bootstrap method for computing singular vector approximations in a systematic way. This is in contrast to the aggregation-based solvers in [1] and [2], where Krylov methods are used as the multigrid smoother, leading to a non-stationary multigrid iteration, and in [22], where a Schwarz alternating procedure is used as the smoother, which has been observed to diverge for linear systems with Wilson matrices.

An outline of the remainder of this paper is as follows. First, in Section 2, we introduce the Wilson discretization of the Dirac equation and discuss some of the features of this problem that make it difficult to solve using iterative methods. Then, in Section 3, we present a Galerkin coarsening algorithm that combines the weighted least squares process for constructing interpolation with bootstrap and adaptive techniques for computing test vectors used in this construction. Section 4 contains numerical results of the proposed method applied to the Wilson discretization of the 2-dimensional Dirac equation. We end with concluding remarks in Section 5.

2. The Wilson discretization of the Dirac equation. In Lattice QCD, the Dirac equation is typically analyzed on a hypercube with periodic (or anti-periodic) boundary conditions. A brief description of the Wilson discretization that is the focus of this paper is given in this section.

Let N_s denote the number of spin components and N_c the number of color components of the fields ψ , then the action of the Wilson matrix D on ψ at a grid point $z \in \Omega = \{1, \dots, N\}^d$, with N the number of grid points in a given space-time dimen-

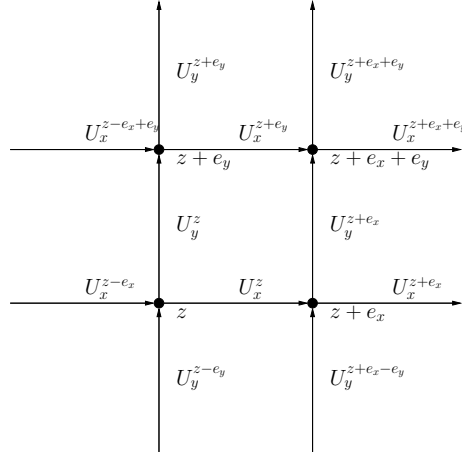


Fig. 2.1: Naming convention on the grid.

sion, reads

$$(D\psi)_z = m_q \psi_z - \sum_{\mu=1}^d \left[(P_\mu^- \otimes U_\mu^z) \psi_{z+e_\mu} + (P_\mu^+ \otimes \bar{U}_\mu^{z-e_\mu}) \psi_{z-e_\mu} \right], \quad (2.1)$$

where $m_q = m + 2(d-1)$ is a scalar quantity, $P_\mu^\pm = \frac{(I \pm \gamma_\mu)}{2}$ satisfy $(P_\mu^\pm)^2 = P_\mu^\pm$, with $\gamma_\mu \in \mathbb{C}^{N_s \times N_s}$ denoting anti-commuting matrices, i.e., $\gamma_\mu \gamma_\nu + \gamma_\nu \gamma_\mu = 2\delta_{\mu,\nu} I_{N_s}$, and $U_\mu^z \in SU(N_c)$ are the discrete gauge fields belonging to the Lie group $SU(N_c)$, $N_c \geq 1$, of $N_c \times N_c$ unitary matrices with determinant equal to one, and e_μ denotes the canonical unit vector in the μ -direction, i.e., $z + e_\mu$ describes a shift from grid point z to its neighbor in the μ -direction. The unknown field, ψ , is defined at the grid points $z \in \Omega$ with $N_s \cdot N_c$ variables per grid point. The discrete gauge fields U_μ^z are defined on the edges of the grid, as illustrated in Figure 2.1 in a 2-dimensional setting. The set $\{U_\mu^z \in SU(N_c), \mu = 1, \dots, d, z \in \Omega\}$ of discrete gauge fields U_μ^z is referred to as a gauge configuration. For a more detailed introduction to QCD and lattice QCD we refer to [19, 23, 29].

In the 2-dimensional setting that we consider in this paper, $N_s = 2$ and $N_c = 1$ so that the γ_μ -matrices are given by

$$\gamma_1 = \begin{pmatrix} 0 & 1 \\ 1 & 0 \end{pmatrix} \quad \text{and} \quad \gamma_2 = \begin{pmatrix} 0 & i \\ -i & 0 \end{pmatrix},$$

and the fields U_z^μ which are defined on the edges of the grid belong to the $U(1)$ group, i.e., they are complex numbers with modulus one. In order to give an explicit expression for the action of D on a field $\psi \in \mathbb{C}^{2N^2}$ we consider a spin-permuted reordering. That is, we write $\psi = (\psi_1^T, \psi_2^T)^T$ where ψ_1 represents the variables with spin 1 at all grid points and ψ_2 represents the variables with spin 2. Ordering D accordingly it has the structure

$$D = \frac{1}{2} \begin{pmatrix} A & B \\ -B^H & A \end{pmatrix}. \quad (2.2)$$

Here, the diagonal blocks, A , are referred to as *Gauge Laplacians*. They were introduced originally by Wilson as a way to stabilize a covariant finite difference discretization of the Dirac equation [36]. The action of $A \in \mathbb{C}^{N^2 \times N^2}$ on a vector $\phi \in \mathbb{C}^{N^2}$ at a grid point $z \in \Omega$ reads

$$(A\phi)_z = (4 + 2m)\phi_z - U_x^{z-e_x}\phi_{z-e_x} - U_y^{z-e_y}\phi_{z-e_y} - \bar{U}_x^z\phi_{z+e_x} - \bar{U}_y^z\phi_{z+e_y},$$

and the action of $B \in \mathbb{C}^{N^2 \times N^2}$ on $\phi \in \mathbb{C}^{N^2}$ at site $z \in \Omega$ is given by

$$(B\phi)_z = \bar{U}_x^z\phi_{z+e_x} - U_x^{z-e_x}\phi_{z-e_x} + i\left(\bar{U}_y^z\phi_{z+e_y} - U_y^{z-e_y}\phi_{z-e_y}\right).$$

We note that if $U_\mu^z = 1$ for $\mu = x, y$ and all $z \in \Omega$, then A is the standard 5-point Laplacian (plus a diagonal shift) and B is a central difference approximation to the gradient of ϕ .

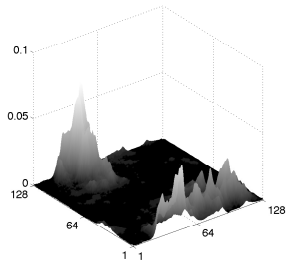
The gauge field configurations used in different calculations throughout the paper are generated using a standard Metropolis algorithm with a quenched Wilson gauge field action

$$S = \sum_{z \in \Omega} \beta \operatorname{Re}(\bar{U}_y^z \bar{U}_x^{z+e_y} U_y^{z+e_x} U_x^z). \quad (2.3)$$

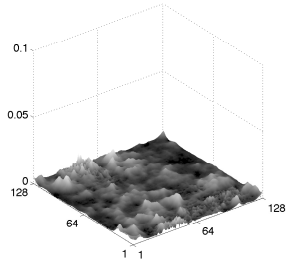
For details on the Metropolis algorithm and its implementation in this setting we refer to [20]. In general, the distribution of the gauge fields depends on the parameter β in (2.3). The case $\beta \rightarrow \infty$ yields $U_\mu^z \rightarrow 1$ for $\mu = x, y$ and all $z \in \Omega$. As $\beta \rightarrow 0$, the phases θ_μ^z in $U_\mu^z = e^{i\theta_\mu^z}$ become less correlated and the gauge fields become highly disordered, causing local oscillations in the near kernel components of the Wilson matrix. In our tests, we consider three values of $\beta = 3, 6, 10$ and nine configurations of the gauge fields for each value, corresponding to steps 11,000, 12,000, ..., 19,000 of a standard Metropolis algorithm using the action given in (2.3). We note that the same configurations are reused in all the tests.

2.1. Singular vectors of the Wilson matrix. One difficulty that arises when designing multigrid solvers for the Wilson discretization of the Dirac equation is that the support and local structure of the near kernel components of the Wilson matrix depend on the local values of the gauge fields. As an example, plots of the modulus of the individual spin components of the right singular vectors to small singular values of D for $N = 128$, $\beta = 6$ at $\eta = 10^{-7}$ are provided in Figures 2.2, 2.3 and 2.4. In this case, which is representative of what happens for physically relevant configurations, the singular vectors belonging to small singular values of the Wilson matrix are locally non-smooth. It is this feature that motivates the use of adaptive AMG techniques for the Wilson matrix.

In addition, we observe that some of the singular vectors to small singular values are localized, e.g., the smallest in Figure 2.2 and 2nd smallest in Figure 2.3. This is in contrast to the singular vector belonging to the 10th smallest singular value shown in Figure 2.4. These findings of non-smooth, localized and non-localized near kernel vectors is indicative of what occurs in practice. Related numerical studies on the local supports of the eigenvectors of the Wilson matrix are found in [26]. Assuming a point-wise smoother, the coarse space basis used in the associated AMG solver for this problem must be able to approximate a large number of (possibly localized) near kernel vectors, which motivates the use of least squares interpolation as a technique for accurately approximating sets of such test vectors collectively.

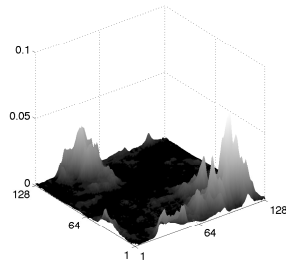


(a) First spin component.

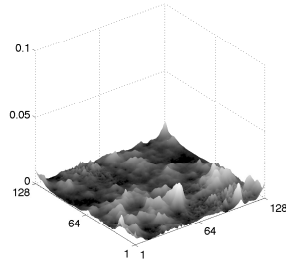


(b) Second spin component.

Fig. 2.2: Modulus of the spin components of the right singular vector to the smallest singular value $\sigma_1 = 8.49 \cdot 10^{-8}$.

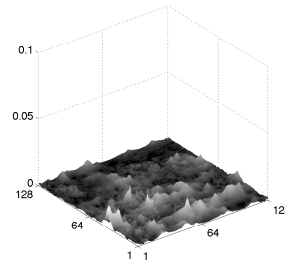


(a) First spin component.

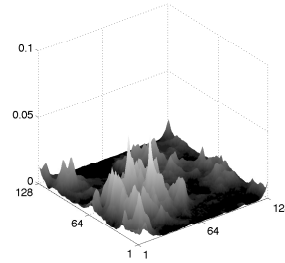


(b) Second spin component.

Fig. 2.3: Modulus of the spin components of the right singular vector to the 2nd smallest singular value $\sigma_2 = 1.65 \cdot 10^{-3}$.



(a) First spin component.



(b) Second spin component.

Fig. 2.4: Modulus of the spin components of the right singular vector to the 10th smallest singular value $\sigma_{10} = 2.09 \cdot 10^{-2}$.

2.2. Spectrum of the Wilson matrix. Representing the near kernel vectors of the Wilson matrix D in the coarse space is further complicated by the fact that in practice the shift m is chosen such that

$$\eta_{\min}(D) = \min_{\lambda \in \text{spec}(D)} \text{Re}(\lambda) \in \mathbb{R}, \quad (2.4)$$

is positive and close to zero, with $\text{spec}(D)$ denoting the spectrum of D . The spectra of the mass-less Wilson matrix D_0 , i.e., (2.1) with $m_q = 2(d-1)$, for $n = 32$ with $\beta = 3$ and $\beta = 6$ are provided in Figure 2.5, and Figure 2.6 contains plots of the 16 smallest eigenvalues of D_0 for $N = 128$ and $\beta = 6$ for nine distinct gauge field configurations. We note that in all cases the eigenvalues of D_0 have a positive real part, which holds for all of the problems considered in this paper. Additionally, as the plots in Figure 2.5 illustrate, when the value of β decreases the eigenvalue with minimal real part moves away from the origin and the eigenvalue with maximal real part moves closer to the origin.

The γ_5 -symmetry of the Wilson matrix implies that the eigenvalues of D are either real or appear in complex conjugate pairs. Specifically, define $\gamma_5 = \text{diag}(1, -1)$

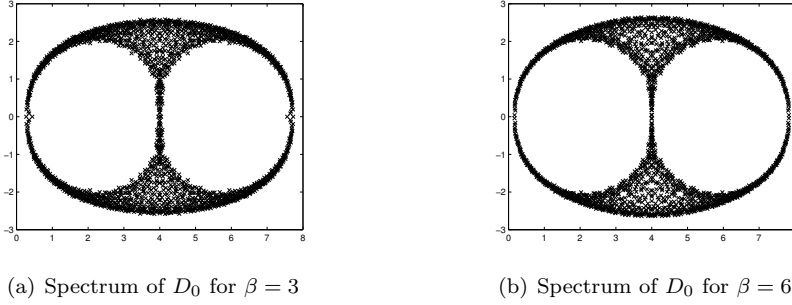


Fig. 2.5: Spectra of the mass-less Wilson matrix D_0 for $N = 32$ and $\beta = 3, 6$, configuration 13,000.

and set $\Gamma_5 = I_{N^2} \otimes \gamma_5$. Then, $\Gamma_5^H \Gamma_5 = \Gamma_5^2 = I$ and

$$\Gamma_5 D = D^H \Gamma_5 \quad \text{or} \quad D = \Gamma_5 D^H \Gamma_5.$$

Now, if v_λ denotes a right eigenvector of D to the eigenvalue $\lambda \neq \bar{\lambda}$, we see that $\Gamma_5 v_\lambda$ is a left eigenvector to the eigenvalue $\bar{\lambda}$, i.e.,

$$D v_\lambda = \lambda v_\lambda \iff (\Gamma_5 v_\lambda)^H D = \bar{\lambda} (\Gamma_5 v_\lambda)^H, \quad (2.5)$$

Thus, to each right eigenpair (λ, v_λ) there corresponds a left eigenpair $(\bar{\lambda}, \Gamma_5 v_\lambda)$, and the spectrum of D is symmetric with respect to the real axis. More generally, since Γ_5 is unitary, we have $\|\Gamma_5 x\|_2 = \|x\|_2$ for any x , and the γ_5 -symmetry yields, in addition, that $\|Dx\|_2 = \|D^H \Gamma_5 x\|_2$. Thus for a general near kernel component, $x \in \mathbb{C}^n$, we find that

$$\frac{\|Dx\|}{\|x\|} \approx 0 \iff \frac{\|D^H \Gamma_5 x\|}{\|\Gamma_5 x\|} \approx 0.$$

Overall, as the plots in Figures 2.5 and 2.6 illustrate, depending on the choice of the shift m , the resulting system matrix can have a large number of eigenvalues that are close to zero and, thus, potentially a large number of small singular values. This observation motivates the use of the multigrid eigensolver as an approach to efficiently compute several near kernel components simultaneously in the proposed bootstrap AMG setup algorithm.

2.3. Failure of Krylov methods for the Wilson matrix. Typically, a standard Krylov method (e.g., BiCG, GMRES, CGNR) is used to solve the linear systems (1.1) arising throughout a lattice QCD simulation. The large condition number of the Wilson matrices that result from physically relevant choices of the shift m lead to slow convergence of these methods, as shown in the plots on the left in Figure 2.7, where we report results of CGNR and restarted GMRES with a restart value of 32 (GMRES(32)) applied to a series of linear systems involving 2-dimensional Wilson matrices. For both methods, we see that the solver requires a large number of iterations to drive the residual down to the given tolerance and that GMRES(32) reaches the maximum number of iterations before reaching the convergence criteria in many cases. Here, the maximum number of iterations is limited to 4096 and the solver stops

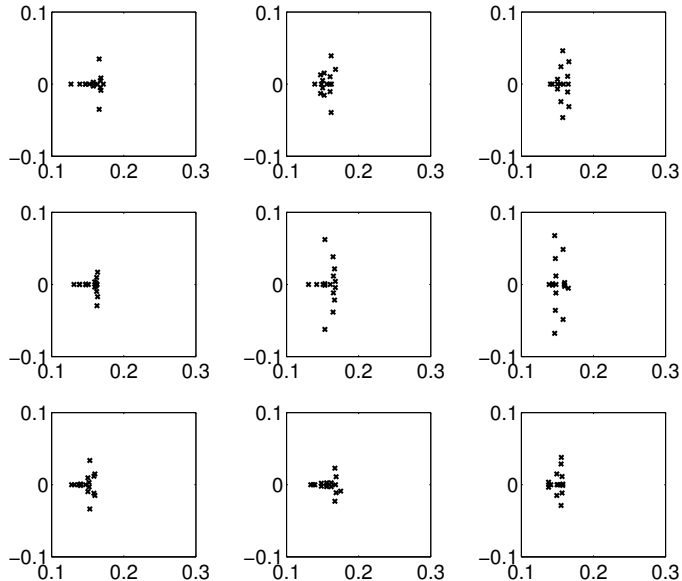


Fig. 2.6: Smallest sixteen eigenvalues of the Wilson matrix D_0 for $N = 128$ and $\beta = 6$. The plots from left to right and then top to bottom correspond to the nine gauge field configurations 11,000, 12,000, ..., 19,000.

if it reaches the prescribed tolerance of 10^{-8} reduction in the relative residual or this number of iterations.

Moreover, as illustrated in the plots on the right in Figure 2.7, even when the algorithm stops successfully, the actual error is large compared to the residual. In fact, we observe that the relative ℓ_2 norm of the error is up to six orders of magnitude larger than the relative ℓ_2 norm of the final residual. Of course, decreasing the tolerance for the norm of the residual for either method should further reduce the error, but would result in an even larger number of iterations. Overall, these results are representative of the performance of standard Krylov methods applied to the Wilson matrix. We mention in addition that although m is set so that $\eta_{\min}(D) > 0$, $\lambda_{\min}(A)$, the smallest eigenvalue of the gauge Laplacian block from (2.2), can become negative which complicates the use of block preconditioners (e.g., Uzawa type schemes) for the solution of Wilson matrices for physically relevant choices of m .

3. Bootstrap geometric-AMG for the Wilson matrix. In this section, we develop a bootstrap approach for linear systems with the non-Hermitian Wilson matrix and study it in detail. The algorithm we consider here combines a bootstrap setup to compute the test vectors used in defining interpolation with an adaptive step that applies the existing solver to an appropriate initial guess to update the test vector(s). We note that all arguments made in this section also carry over to other discretizations of the Dirac equation as long as they satisfy the γ_5 -symmetry.

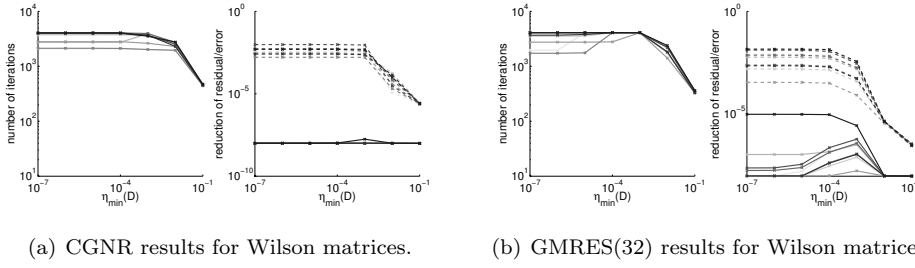


Fig. 2.7: Results of CGNR and GMRES(32) applied to Wilson matrices for $N = 128$ and $\beta = 6$. The results for the light to dark lines correspond to different gauge field configurations, going from light to dark with increasing configuration number. On the left of each subplot, the number of iterations needed to reduce the ℓ_2 norm of the relative residual by a factor 10^{-8} is plotted against different values of $\eta_{\min}(D)$ defined in (2.4), corresponding to different choices of the diagonal shift m . On the right of each subplot, the resulting relative residuals (solid lines) and relative errors (dashed lines) are plotted against $\eta_{\min}(D)$.

3.1. Kaczmarz relaxation. As the smoother in the proposed BAMG algorithm we consider Kaczmarz relaxation. For the linear system, $D\psi = b$, with the non-Hermitian Wilson matrix D the Kaczmarz iteration is based on the equivalent formulation involving the normal equations

$$D^H D\psi = D^H b. \quad (3.1)$$

Given an approximation to the solution, ψ , of (3.1), one iteration of the basic Kaczmarz iteration for this formulation reads:

$$\psi \leftarrow \psi + s_i e_i, \quad i = 1, \dots, n,$$

where e_i is the i -th Euclidian basis vector and s_i is chosen so that the corresponding component of the residual vanishes:

$$\langle D^H b - D^H D(\psi + s_i e_i), e_i \rangle = 0.$$

Now, setting $r = b - D\psi$ gives

$$\langle D^H(r + s_i D e_i), e_i \rangle = 0, \quad \text{implying} \quad s_i = \frac{\langle r, D e_i \rangle}{\|D e_i\|_2^2}.$$

Thus in practice Kaczmarz relaxation can be realized using column access to the entries of D only and the arithmetic complexity of a single iteration depends only on the number of non-zero entries in D .

Local mode analysis for Kaczmarz relaxation suggests that it is widely applicable as a smoother, although it is often less efficient with respect to the actual smoothing rate (see [34, Section 4.7]). Further analysis of the smoothing properties of the Kaczmarz iteration applied to general rectangular systems is found in [31]. While local mode analysis is not applicable to the Wilson matrix due to the local variations in the gauge fields and, hence, its off-diagonal entries, the numerical results we provide

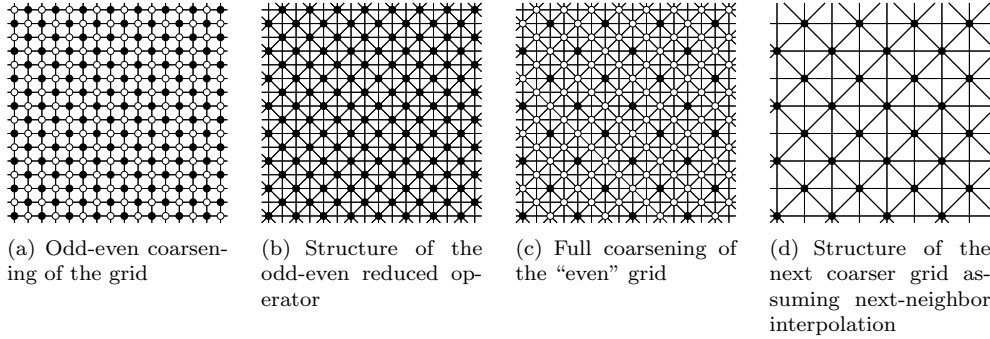


Fig. 3.1: The odd-even reduction and full coarsening of the grid of even points. The circles denote grid points and the edges connections among them, defined according to the graph of D and the Schur complement \widehat{D} resulting from odd-even reduction. In (a) and (c) white points correspond to coarse points.

for the proposed multigrid solver with Kaczmarz smoother suggest its robustness for the Wilson discretization of the Dirac equation. We address its suitability in the bootstrap AMG setup process for computing singular value triplets in the subsequent section.

We note that the Kaczmarz iteration as defined above updates the unknowns in sequential order $i = 1, \dots, N^d$, referred to as a *forward sweep*. Thus, as is, the method is not amenable to parallel computing. Formulating a parallel version using an appropriate *coloring* strategy to order the updates of the unknowns is, however, straightforward since Wilson's discretization of the Dirac equation is formulated on a regular grid with nearest-neighbor coupling.

3.2. Geometric coarsening. The nearest-neighbor finite difference scheme and regular cubic grid used in the Wilson discretization of the Dirac equation allows for an odd-even reduction (or coarsening), which is typically applied when developing solvers for this system [2, 21]. Let a grid point $(x, y) \in \{1, \dots, N\}^2$ be labeled as *even* if $x + y$ is even and as *odd* otherwise (see Fig. 3.1). In case the total number of grid points, n , is even, then the number of odd and even points is exactly $n/2$. Any vector $\psi \in \mathbb{C}^n$ can be written as $\psi = (\psi_e^T, \psi_o^T)^T$ by numbering the even points before the odd ones. Using the same numbering scheme for the rows and columns of the Wilson matrix gives

$$D = \begin{pmatrix} D_{ee} & D_{eo} \\ D_{oe} & D_{oo} \end{pmatrix}.$$

Now, since D couples only nearest-neighbors on the grid (see Fig. 3.1 (a)), the blocks D_{ee} and D_{oo} are diagonal. Specifically, $D_{ee} = D_{oo} = c \cdot I$ for $c \in \mathbb{R}$ and upon scaling by c^{-1} the constant can be set as $c = 1$. Define the operator

$$\widehat{D} = I - D_{eo}D_{oe}, \quad (3.2)$$

i.e., \widehat{D} is the the Schur complement of D with respect to the even points, referred to as the odd-even reduced matrix. With it the solution of the linear system $D\psi = b$ can be calculated in the following two steps.

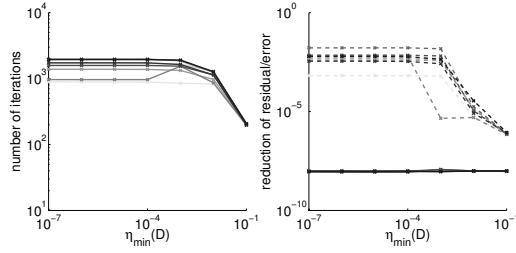


Fig. 3.2: Results of CGNR applied to the odd-even reduced system with $N = 128$ and $\beta = 6$. The results for the light to dark lines correspond to different gauge field configurations, going from light to dark with increasing configuration number. On the left, the number of iterations needed to reduce the relative residual by a factor 10^{-8} is plotted against $\eta_{\min}(D)$ defined in (2.4), corresponding to different diagonal shifts m . On the right, the resulting relative residuals (solid lines) and relative errors (dashed lines) are plotted against $\eta_{\min}(D)$.

1. Solve $\widehat{D}\psi_e = b_e - D_{eo}b_o$.
2. Compute $\psi_o = \psi_o - D_{oe}x_e$.

From the form of the Schur complement in (3.2), we see that a matrix vector multiplication with \widehat{D} requires roughly the same number of floating point operations as the multiplication with D . However, solving systems with \widehat{D} , instead of the original matrix D , typically reduces the total number of CGNR iterations by a factor of two. This is illustrated in Figure 3.2, where results of CGNR applied to the system with \widehat{D} for $N = 128$ and $\beta = 6$ are reported. Here, we use the same nine gauge configurations considered in the tests of CGNR applied to the unreduced Wilson matrix D reported in Figure 2.7 and we see that CGNR applied to \widehat{D} needs half as many iterations on average in order to reduce the ℓ_2 norm of the relative residual by the factor 10^{-8} .

Since CGNR for the system with \widehat{D} is the default solver in various lattice QCD simulation codes [2, 21], our construction of the proposed BAMG algorithm is based on the odd-even reduced matrix \widehat{D} . Fig. 3.1 (c) illustrates the full coarsening strategy we use for \widehat{D} on the first even (coarse) grid and on all subsequent grids of the AMG hierarchy, namely, we define every other grid point in every dimension as a coarse grid point. Now, if in addition nearest-neighbor (restriction and) interpolation and a (Petrov) Galerkin coarse-grid construction are used, then it follows that the resulting coarse-grid operator again has the same sparsity structure, as depicted in Fig. 3.1 (d).

An important observation for the derivation of the bootstrap setup cycle presented in the next section is that the Schur complement on the even grid also satisfies the γ_5 -symmetry, so that the results we present for D hold for \widehat{D} as well. To see that \widehat{D} satisfies the γ_5 -symmetry, consider the corresponding block form of Γ_5 , i.e.,

$$\Gamma_5 = \begin{pmatrix} \Gamma_o & \\ & \Gamma_e \end{pmatrix},$$

where Γ_o, Γ_e have the same structure as Γ_5 . Direct computation shows that we have $D_{oe}^H \Gamma_o = \Gamma_e D_{eo}$, $D_{eo}^H \Gamma_e = D_{oe} \Gamma_o$ and, thus,

$$\widehat{D}^H \Gamma_e = \Gamma_e \widehat{D}. \quad (3.3)$$

3.3. Least squares restriction and interpolation. The first main component of the bootstrap AMG algorithm is its use of a least squares process to form the restriction and interpolation operators. The least squares restriction R and interpolation P are defined to fit collectively sets of left and right test vectors, respectively. The test vectors used in these fits characterize the near kernel of the system matrix. In order to simplify notation, we present the least squares process first in a more general setting, i.e., for general sets of interpolatory variables \mathcal{C}_i , and then discuss the specific definition we use in the proposed algorithm, which we base on the block-spin structure of the Wilson matrix given in (2.2). Further, we present only the construction of P and note that R^H is obtained in complete analogy.

Let $\widehat{\Omega}$ denote the set of all variables of the linear system (1.1), then given a set of coarse variables $\mathcal{C} \subset \widehat{\Omega}$, e.g., defined by full coarsening, we set $\mathcal{F} = \widehat{\Omega} \setminus \mathcal{C}$. Further, let the set of interpolatory variables for a fine variable $i \in \mathcal{F}$ be denoted by \mathcal{C}_i , typically consisting of neighboring coarse variables. Then the structure of P is defined by

$$P_{ij} = 0 \text{ for } j \notin \mathcal{C}_i.$$

Once the sets of interpolatory variables, \mathcal{C}_i , and a set of test vectors, $\mathcal{V} = \{\tilde{v}^{(1)}, \dots, \tilde{v}^{(k)}\} \subset \mathbb{C}^n$, have been determined, the i th row of P for $i \in \mathcal{F}$, denoted by p_i , is then defined as the minimizer of the local least squares problem:

$$\mathcal{L}(p_i) = \sum_{\kappa=1}^k \omega_{\kappa} \left(\tilde{v}_{\{i\}}^{(\kappa)} - \sum_{j \in \mathcal{C}_i} (p_i)_j \tilde{v}_{\{j\}}^{(\kappa)} \right)^2 \mapsto \min. \quad (3.4)$$

Here, the notation $\tilde{v}_{\widehat{\Omega}}$ denotes the canonical restriction of the vector \tilde{v} to the set $\widehat{\Omega} \subset \widehat{\Omega}$, e.g., $\tilde{v}_{\{i\}}$ is simply the i th entry of \tilde{v} . The weights $\omega_{\kappa} > 0$ are chosen to reflect the importance of the corresponding test vector (e.g., its A -norm $\|\tilde{v}\|_A^2 = \langle A\tilde{v}, \tilde{v} \rangle$ when A is Hermitian and positive definite). We give our specific choice of the weights in the next section. Conditions on the uniqueness of the solution to minimization problem (3.4) and an explicit form of the minimizer have been derived in [7].

In the case where there is more than one variable per grid point¹, the interpolatory sets used in the least squares process are defined as follows. The sets \mathcal{F} and \mathcal{C} are defined with respect to grid points rather than variables. That is, all variables at a given grid point are marked either fine or coarse collectively. Then, given a grid point $i \in \mathcal{F}$ with associated variables i_1, \dots, i_m , interpolation is built independently for each variable. The set of interpolatory variables \mathcal{C}_{i_*} for each variable is then composed of a subset or all of the variables defined at grid points $j \in \mathcal{C}$ in the neighborhood of grid point i . In the following sections, we show that by imposing further conditions on the sets of interpolatory variables \mathcal{C}_{i_*} it is possible to preserve the spin structure and γ_5 -symmetry on coarse grids, which is an important feature in our proposed bootstrap setup algorithm.

3.4. The bootstrap multigrid setup cycle. The second main component of the bootstrap AMG setup is the bootstrap cycle used for computing the test vectors that are needed in the least squares interpolation process (3.4). The proposed bootstrap cycle setup uses two complementary processes to compute the sets of tests vectors:

¹This is the case for the 2-dimensional Wilson matrix where two variables, corresponding to the two spin components, are defined at each grid point.

1. a solver applied to appropriately formulated homogenous problems on different grids, as in adaptive AMG,
2. a multigrid eigensolver.

As discussed in detail below, the main idea in the latter multigrid eigensolver is to use appropriate mass matrices to formulate generalized eigenproblems on coarser grids in such a way that these generalized eigenproblems can be directly related to the finest-grid eigenproblem.

Following the reasoning in Section 1, we use the fact that these smooth error components are characterized by left and right singular vectors with small singular values. That is, in analogy to the Hermitian and positive definite case, we seek to construct test vectors that capture the algebraically smooth components of the error, i.e., vectors x such that $Dx \approx 0$ or $D^H x \approx 0$. Let $D = U\Sigma V^H$ be the SVD of the non-Hermitian Wilson matrix D , where $U = [u_1 \mid \dots \mid u_n] \in \mathbb{C}^{n \times n}$ and $V = [v_1 \mid \dots \mid v_n] \in \mathbb{C}^{n \times n}$ are unitary matrices. Then, the left and right singular vectors and corresponding singular values are given by the triplets (σ_i, u_i, v_i) that satisfy the equations

$$\begin{aligned} Dv_i &= \sigma_i u_i, \\ D^H u_i &= \sigma_i v_i. \end{aligned}$$

Now, since these equations are equivalent to the Hermitian and indefinite eigenvalue problem (cf. [24, 27])

$$\begin{pmatrix} & D \\ D^H & \end{pmatrix} \begin{pmatrix} U & U \\ V & -V \end{pmatrix} = \begin{pmatrix} U & U \\ V & -V \end{pmatrix} \begin{pmatrix} \Sigma & \\ & -\Sigma \end{pmatrix}, \quad (3.5)$$

it follows that a Petrov Galerkin bootstrap AMG process for the non-Hermitian matrix D can be reformulated as a Galerkin bootstrap AMG process for the Hermitian system (3.5), to which the algorithm developed in [7] can be applied. This approach was proposed for the computation of singular triplets in [33] and is described in the following.

Starting with the finest-grid system D_1 , the Petrov Galerkin bootstrap setup cycle begins by applying relaxation (e.g., Kaczmarz iterations) to the homogeneous systems

$$D_l \tilde{v}_i^{(\kappa)} = 0, \quad \text{and} \quad D_l^H \tilde{u}_i^{(\kappa)} = 0, \quad \kappa = 1, \dots, k_r, \quad l = 1, \dots, L-1, \quad (3.6)$$

to compute some initial sets of right $\mathcal{V}_l^r = \{\tilde{v}_i^{(\kappa)}, \kappa = 1, \dots, k_r\}$ and left $\mathcal{U}_l^r = \{\tilde{u}_i^{(\kappa)}, \kappa = 1, \dots, k_r\}$ test vectors used in constructing the least squares interpolation P_{l+1}^l and restriction R_l^{l+1} operators, $l = 1, \dots, L-1$, respectively, and thereby also the corresponding coarse-grid operators. On the finest grid, k_r distinct random vectors are used as the initial guesses for the Kaczmarz iterations applied to each of the two systems in (3.6). On all subsequent grids except the coarsest, $l = 1, \dots, L-1$, the resulting relaxed vectors computed on finer grids l are restricted to the coarser grids $l+1$ and used as the initial guesses for Kaczmarz applied to the two systems in (3.6) there.

Once such an initial multigrid hierarchy has been constructed, the current sets of test vectors are updated with approximations of the near kernel that are computed using a bootstrap multigrid eigensolver based on the existing multigrid structure. The bootstrap multigrid eigensolver begins by computing the k_e left and right singular vectors with the smallest singular values of a generalized SVD for the coarsest grid

operator, D_L . More specifically, define the composite restriction and interpolation operators for $l = 2, \dots, L$ by

$$\begin{aligned} P_l &= P_2^1 \cdot \dots \cdot P_l^{l-1}, \\ R_l &= R_{l-1}^l \cdot \dots \cdot R_1^2, \end{aligned}$$

and correspondingly the coarse-grid operators and associated mass matrices by $D_l = R_l D P_l$, $Q_l = R_l R_l^H$, and $T_l = P_l^H P_l$. The triplets $(\tilde{\sigma}_L^{(\kappa)}, \tilde{u}_L^{(\kappa)}, \tilde{v}_L^{(\kappa)})$, $\kappa = 1, \dots, k_e$, corresponding to the k_e smallest singular values of the coarsest-grid system are then computed by solving the generalized singular value problem

$$D_L \tilde{v}_L^{(\kappa)} = \tilde{\sigma}_L^{(\kappa)} Q_L \tilde{u}_L^{(\kappa)}, \quad (3.7)$$

$$D_L^H \tilde{u}_L^{(\kappa)} = \tilde{\sigma}_L^{(\kappa)} T_L \tilde{v}_L^{(\kappa)}. \quad (3.8)$$

We note that, since the size of the coarsest-grid system matrix D_L is small, these triplets can be computed directly by solving the equivalent generalized Hermitian (indefinite) eigenvalue problem on the coarsest grid given by

$$\begin{pmatrix} D_L^H & D_L \end{pmatrix} \begin{pmatrix} \tilde{U} & \tilde{U} \\ \tilde{V} & -\tilde{V} \end{pmatrix} = \begin{pmatrix} Q_L & \\ & T_L \end{pmatrix} \begin{pmatrix} \tilde{U} & \tilde{U} \\ \tilde{V} & -\tilde{V} \end{pmatrix} \begin{pmatrix} \tilde{\Sigma} & \\ & -\tilde{\Sigma} \end{pmatrix}, \quad (3.9)$$

where the diagonal entries of $\tilde{\Sigma}$ contain the ordered approximate singular values. Note, that (3.9) is obtained from (3.5) by a Galerkin construction using the interpolation operator

$$\hat{P}_L = \begin{pmatrix} R_L & \\ & P_L \end{pmatrix}.$$

The following observation guides the construction of the bootstrap multigrid eigensolver: If $(\tilde{\sigma}_l^{(\kappa)}, \tilde{u}_l^{(\kappa)}, \tilde{v}_l^{(\kappa)})$ is a triplet of the finer grid SVD and if there exist coarse-grid vectors $\tilde{u}_{l+1}^{(\kappa)}$ and $\tilde{v}_{l+1}^{(\kappa)}$ such that $\tilde{u}_l^{(\kappa)} = R_{l+1}^l \tilde{u}_{l+1}^{(\kappa)}$ and $\tilde{v}_l^{(\kappa)} = P_{l+1}^l \tilde{v}_{l+1}^{(\kappa)}$, then $(\tilde{\sigma}_{l+1}^{(\kappa)}, \tilde{u}_{l+1}^{(\kappa)}, \tilde{v}_{l+1}^{(\kappa)})$ is a triplet on the coarse-grid, i.e.,

$$R_{l+1}^{l+1} D_l P_{l+1}^l \tilde{v}_{l+1}^{(\kappa)} = \tilde{\sigma}_{l+1}^{(\kappa)} Q_l \tilde{u}_{l+1}^{(\kappa)},$$

and, with $P_l^{l+1} := (P_{l+1}^l)^H$,

$$P_l^{l+1} D_l^H R_{l+1}^l \tilde{u}_{l+1}^{(\kappa)} = \tilde{\sigma}_{l+1}^{(\kappa)} T_l \tilde{v}_{l+1}^{(\kappa)}.$$

This result gives a relation among the singular triplets computed in the bootstrap setup on all grids, which we now use to derive a multigrid eigensolver for the Hermitian system (3.5). On finer grids, starting with $l = L - 1$, we define a smoother for the systems

$$D_l \tilde{v}_l^{(\kappa)} = \tilde{\sigma}_l^{(\kappa)} Q_l \tilde{u}_l^{(\kappa)}, \quad (3.10)$$

$$D_l^H \tilde{u}_l^{(\kappa)} = \tilde{\sigma}_l^{(\kappa)} T_l \tilde{v}_l^{(\kappa)}, \quad (3.11)$$

by a scheme that applies the Kaczmarz iteration to each of these two systems separately, alternating between the two. Here, the singular value approximations $\tilde{\sigma}_l^{(\kappa)}$ are updated after each such alternating sweep as

$$\tilde{\sigma}_l^{(\kappa)} = \frac{\langle D_l \tilde{v}_l^{(\kappa)}, \tilde{u}_l^{(\kappa)} \rangle}{\langle Q_l \tilde{u}_l^{(\kappa)}, \tilde{u}_l^{(\kappa)} \rangle^{\frac{1}{2}} \langle T_l \tilde{v}_l^{(\kappa)}, \tilde{v}_l^{(\kappa)} \rangle^{\frac{1}{2}}}, \quad \kappa = 1, \dots, k_e. \quad (3.12)$$

After several such sweeps, the resulting approximations are normalized with respect to the mass matrices

$$\tilde{v}_l^{(\kappa)} = \frac{\tilde{v}_l^{(\kappa)}}{\langle T_l \tilde{v}_l^{(\kappa)}, \tilde{v}_l^{(\kappa)} \rangle^{\frac{1}{2}}} \quad \text{and} \quad \tilde{u}_l^{(\kappa)} = \frac{\tilde{u}_l^{(\kappa)}}{\langle Q_l \tilde{u}_l^{(\kappa)}, \tilde{u}_l^{(\kappa)} \rangle^{\frac{1}{2}}}.$$

They are then added to the sets of right and left test vectors

$$\begin{aligned} \mathcal{U}_l &= \mathcal{U}_l^r \cup \mathcal{U}_l^e \quad \text{with} \quad \mathcal{U}_l^e := \{\tilde{u}_l^{(\kappa)}, \kappa = 1, \dots, k_e\}, \\ \mathcal{V}_l &= \mathcal{V}_l^r \cup \mathcal{V}_l^e \quad \text{with} \quad \mathcal{V}_l^e := \{\tilde{v}_l^{(\kappa)}, \kappa = 1, \dots, k_e\}, \end{aligned}$$

which are used to recompute R_{l+1}^l and P_{l+1}^l , respectively, using the least squares process. Here, the superscripts r and e are used to distinguish between the sets of test vectors resulting from applying Kaczmarz relaxation to the homogenous problems (3.6) and the sets of test vectors coming from the Kaczmarz iterations applied to (3.10) and (3.11), with initial guesses coming from solutions to the coarsest-grid eigenproblem (3.9).

3.5. The γ_5 -symmetry and Galerkin coarsening. A Galerkin coarsening scheme for the non-Hermitian Wilson matrix was first considered in the context of an adaptive aggregation-based multigrid solver in [1]. The idea was motivated by the γ_5 -symmetry of the Wilson matrix. Recall that, by (2.5) for each eigenpair (λ, v_λ) there corresponds a left eigenpair $(\bar{\lambda}, \Gamma_5 v_\lambda)$. This motivates the choice $R_1^2 = (\Gamma_5 P_2^1)^H$ on the finest grid. Maintaining a similar relation $R_l^{l+1} = (\Gamma_{5,l} P_{l+1}^l)^H$ on all coarser grids means that the coarse grid system should satisfy

$$\Gamma_{5,l+1} D_{l+1} = D_{l+1}^H \Gamma_{5,l+1},$$

with $\Gamma_{5,l+1}$ a unitary and Hermitian matrix inherited from $\Gamma_{5,l}$ on grid l . This is achieved in a Galerkin approach, i.e., $D_{l+1} = (P_{l+1}^l)^H D_l P_{l+1}^l$, if interpolation satisfies

$$\Gamma_{5,l} P_{l+1}^l = P_{l+1}^l \Gamma_{5,l+1}, \quad (3.13)$$

which, in turn, is fulfilled if we enforce that each variable only interpolates from variables of the same spin. In other words, we fix the sparsity of interpolation according to the spin ordering of $\Gamma_{5,l}$ and $\Gamma_{5,l+1}$ as

$$P_{l+1}^l = \begin{pmatrix} * & \\ & * \end{pmatrix}, \quad (3.14)$$

which gives $\Gamma_{5,l} = \gamma_5 \otimes I_{n_l}$. In the context of full coarsening of the grid, as defined in Section 3.2, for each grid point $i \in \mathcal{F}$ we obtain the structure in (3.14) if we define the interpolatory sets for the two spin variables i_1 and i_2 at grid point i independently as

$$\mathcal{C}_{i_*} = \left\{ j_* \in \mathcal{C} \mid D_{i_*, j_*} \neq 0 \right\}. \quad (3.15)$$

In this way, a given spin variable i_* at grid point i interpolates only from variables j_* of the same spin defined at neighboring grid points j . Using these assumptions, direct computation shows that the Petrov Galerkin coarse-grid correction reduces to a Galerkin correction for D (cf. [1]), i.e., for $R_l^{l+1} = (\Gamma_{5,l} P_{l+1}^l)^H$ we have

$$P_{l+1}^l (R_l^{l+1} D_l P_{l+1}^l)^{-1} R_l^{l+1} = P_{l+1}^l \left((P_{l+1}^l)^H D_l P_{l+1}^l \right)^{-1} (P_{l+1}^l)^H.$$

This same structure preserving form of P and the γ_5 -symmetry of D imply, in addition, the equivalence of the Petrov Galerkin bootstrap AMG setup for D and a Galerkin approach for the Hermitian indefinite matrix $Z = \Gamma_5 D$ as we are going to show next.

Indeed, since Z is Hermitian there exists a unitary matrix $V \in \mathbb{C}^{n \times n}$ such that

$$Z = \Gamma_5 D = V \Lambda V^H$$

with $\Lambda = \text{diag}(\lambda_1, \dots, \lambda_n)$, which directly implies

$$D = \Gamma_5 V \text{sign}(\Lambda) |\Lambda| V^H. \quad (3.16)$$

Thus, $U = \Gamma_5 V \text{sign}(\Lambda)$, $V = V$ are unitary and with $S = |\Lambda|$ we have found an expression for the SVD of D in terms of eigenvectors and eigenvalues of Z . This relation implies that the space spanned by any pair of right and left singular vectors u_i, v_i satisfies

$$\text{span}(u_i) = \text{span}(\Gamma_5 v_i),$$

since the factor $\text{sign}(\lambda_i)$ does not change the span. This result is also true for any pair of subspaces spanned by a collection of pairs of singular vectors. As a consequence, the choice $R_i^{l+1} = (\Gamma_{5,l} P_{l+1}^l)^H$, which was motivated in [1] by the correspondence between left and right eigenvectors with respect to the γ_5 -symmetry, is now justified in terms of left and right singular vectors, assuming that P_{l+1}^l is constructed from test vectors approximating right singular vectors to small singular values. Additionally, we have the following new results relating the setup for D and Z .

THEOREM 3.1. *Assume that $R_i^{l+1} = (\Gamma_{5,l} P_{l+1}^l)^H$ and P_{l+1}^l has the block structure defined in (3.14) such that $\Gamma_{5,l} P_{l+1}^l = P_{l+1}^l \Gamma_{5,l+1}$. Then, the two equations (3.10) and (3.11) are equivalent to*

$$Z_l \tilde{v}_i^{(\kappa)} = \tilde{\lambda}_i^{(\kappa)} T_l \tilde{v}_i^{(\kappa)}, \quad \text{with} \quad \tilde{u}_i^{(\kappa)} = \Gamma_{5,l} \tilde{v}_i^{(\kappa)},$$

where $Z_l = \Gamma_{5,l} D_l$. Thus, in particular, we have the following equivalences.

- (i) *The singular-value problem on the coarsest grid given by (3.7) and (3.8) is equivalent to the generalized eigenproblem*

$$Z_L \tilde{V} = T_L \tilde{V} \tilde{\Lambda}, \quad \text{where} \quad Z_L = \Gamma_{5,L} D_L \tilde{V}.$$

- (ii) *Kaczmarz relaxation applied to either of the equations (3.10) or (3.11) reduces to applying Kaczmarz to the equation*

$$Z_l \tilde{v}_i^{(\kappa)} = \tilde{\lambda}_i^{(\kappa)} T_l \tilde{v}_i^{(\kappa)}.$$

More precisely, the correction s_i used in the Kaczmarz updates for the systems with D_l , defined via the equation

$$\left\langle D_l^H \left[\tilde{\lambda}_i^{(\kappa)} T_l \Gamma_{5,l} \tilde{v}_i^{(\kappa)} - D_l (\tilde{v}_i^{(\kappa)} + s_i e_i) \right], e_i \right\rangle = 0,$$

can equivalently be computed using the equation for s_i in terms of Z_l given by

$$\left\langle Z_l \left[\tilde{\lambda}_i^{(\kappa)} T_l \tilde{v}_i^{(\kappa)} - Z_l (\tilde{v}_i^{(\kappa)} + s_i e_i) \right], e_i \right\rangle = 0.$$

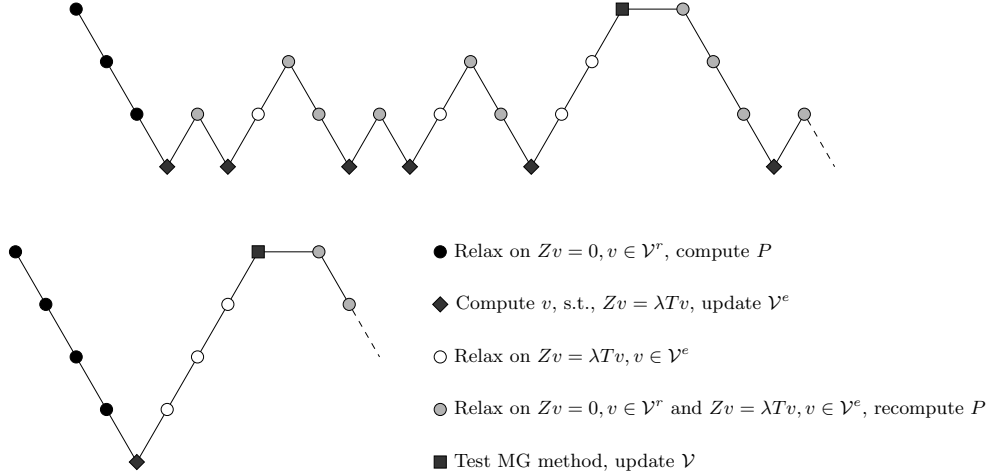


Fig. 3.3: Galerkin Bootstrap AMG W cycle and V cycle setup schemes.

(iii) The singular value approximations defined in (3.12) satisfy $\tilde{\sigma}_l^{(\kappa)} = |\tilde{\lambda}_l^{(\kappa)}|$, where $\tilde{\lambda}_l^{(\kappa)}$ is the Ritz value

$$\tilde{\lambda}_l^{(\kappa)} = \frac{\langle Z_l \tilde{v}_l^{(\kappa)}, \tilde{v}_l^{(\kappa)} \rangle}{\langle T_l \tilde{v}_l^{(\kappa)}, \tilde{v}_l^{(\kappa)} \rangle}. \quad (3.17)$$

Proof. Since $R_l^{l+1} = (\Gamma_{5,l} P_{l+1}^l)^H$ we have $Q_l = T_l$. Now, using (3.16) we have

$$\tilde{u}_l^{(\kappa)} = \text{sign}(\tilde{\lambda}_l^{(\kappa)}) \Gamma_{5,l} \tilde{v}_l^{(\kappa)} \quad \text{and} \quad \tilde{\sigma}_l^{(\kappa)} = \text{sign}(\tilde{\lambda}_l^{(\kappa)}) \tilde{\lambda}_l^{(\kappa)}.$$

Parts (i)–(iii) now follow by substitution. \square

This theorem implies that the overall Petrov Galerkin bootstrap AMG setup process developed for the non-Hermitian Wilson matrix D in Section 3.4 is equivalent to a Galerkin setup process for the Hermitian form of the Wilson matrix Z . We provide additional details of the Galerkin bootstrap setup and multigrid eigensolver for Z in Figure 3.3.

4. Numerical results. In this section, we present numerical tests of our Galerkin bootstrap AMG setup algorithm for the Wilson discretization of the Dirac equation. We apply our method to the Schur complement system resulting from an odd-even reduction of the Wilson matrix:

$$\hat{D}\psi_e = b_e - D_{eo}b_o,$$

with \hat{D} defined as in (3.2), i.e., $D_1 := \hat{D}$. In all tests, the sets of coarse variables are defined by full coarsening (see Figure 3.1). We use nearest neighbor interpolation defined in terms of the graph of the matrix \hat{D} , as in (3.15) which preserves the spin-structure of the system. The maximal number of interpolatory points is bounded by four and the Galerkin coarse-grid operator has the same sparsity pattern on all grids, with at most 18 non-zeros per row and, thus, the grid and operator complexities (cf. [34]) are bounded by 1.4 independent of the problem size.

Fixing the coarsening and sparsity pattern of P as such, we study the performance of the bootstrap algorithm applied to the Hermitian and indefinite matrix $\Gamma_e \widehat{D}$ in (3.3) for $N = 128$ and 256 with $\beta = 3, 6, 10$ in (2.3) and various choices of the shifts, m , used in setting the minimal eigenvalue of the Wilson matrix $D = mI + D_0$. For completeness, we consider nine distinct gauge field configurations for each pair of parameters m and β . In the plots, the (dashed) lines from light to dark correspond to increasing configuration numbers, from 11,000, ..., 19,000, respectively.

The weighted least squares approach in (3.4) is used to define the entries of the interpolation operators. We set the number of test vectors computed using relaxation as $k_r = |\mathcal{V}_r| = 8$ and the number of additional eigenvector approximations computed in the multigrid eigensolver as $k_e = |\mathcal{V}_e| = 8$. The least squares form of P is then computed on each grid using the combined sets of up to $k = k_r + k_e$ test vectors (the initial hierarchy is constructed using only k_r test vectors). On the finest grid, the vectors, $v^{(1)}, \dots, v^{(k_r)}$, used to initialize the bootstrap process, are generated randomly and independently with a normal distribution with expectation zero and variance one.

We use a $W(4, 4)$ cycle solve phase with Kaczmarz smoothing. The problem is coarsened to a coarsest-grid system with $N = 16$, which is solved directly, giving 4- and 5-grid methods for the $N = 128$ and $N = 256$ problem sizes, respectively. The reported estimates of asymptotic convergence rates, ρ , of the resulting solver are computed by

$$\rho = \frac{\|e^\nu\|}{\|e^{\nu-1}\|},$$

where e^ν denotes the error after ν multigrid iterations, i.e., the asymptotic convergence rate is measured upon convergence to the specified tolerance or after $\nu = 100$ iterations. The number of BAMG preconditioned GMRES(32) iterations needed to reduce the ℓ_2 norm of the relative residual to this same tolerance is also reported.

4.1. The 2D Wilson matrix – Bootstrap W cycle setup . In our first set of tests, we use a $W(10,10)$ cycle with Kaczmarz relaxation in the first bootstrap setup cycle. Then, after an intermediate adaptive step in which we apply two $W(4,4)$ cycles to update the test vector with the smallest value of $|\widetilde{\lambda}_0^{(\kappa)}|$ in (3.17) on the finest grid only, we apply a second $W(5,5)$ setup cycle to update the sets of test vectors on all grids which are used to compute the final multigrid hierarchy. After extensive testing of the proposed setup approach, we found these settings to yield a robust solver for all test problems considered. A few remarks regarding these choices of the settings for the setup algorithm are in order before presenting the results of these experiments.

First, we note that the extra smoothing steps are applied in the initial W cycle since we have observed in practice that this gives a sufficiently accurate initial hierarchy from which the solver can then be constructed. Generally, using fewer relaxation steps and a larger number of bootstrap setup cycles is less efficient than an approach in which more relaxation steps are used in each of the cycles, so that fewer cycles are needed to obtain a suitable solver. Moreover, for the highly ill-conditioned Wilson matrices we consider, we find that at least two bootstrap cycles with one intermediate adaptive step is needed in order to obtain an efficient solver for all test problems, unless we increase the number of relaxations that are used in the initial bootstrap cycle significantly.

Additionally, we mention that the intermediate adaptive step is applied only to a single test vector, namely, the one that yields the smallest value of $|\widetilde{\lambda}_0^{(\kappa)}|$ in (3.17) .

While we use this step in all tests, we have observed that it turns out to be beneficial mostly in cases where the shift is chosen such that $\eta_{\min}(D)$ in (2.4) is almost zero, i.e., for the most ill-conditioned cases. In such cases, this simple modification to the algorithm reduces the number of bootstrap setup cycles needed to obtain an efficient solver by at least one and in most cases two or more, assuming the number of smoothing steps are not increased.

As a final remark, we comment that the use of W cycles as opposed to V cycles in the setup and solve phases of the algorithm is needed to compensate for the fact that the problem is coarsened to $N = 16$ and that the maximum number of interpolation variables is limited to four. We observed that for certain realizations of the gauge fields, the resulting coarsest spaces as defined in our algorithm are too lean to compensate for the large number of near kernel vectors that they have to approximate. An alternative strategy, that we did not explore here, would be to increase the number of interpolation points on coarser grids.

The results of these experiments for $N = 128$ are reported in Figure 4.1 and the ones in Figure 4.2 are for $N = 256$. For both problem sizes we report results for $\beta = 3, 6, 10$ for nine different gauge field configurations. Here, we see that for both problem sizes, the stand-alone solver is convergent and only in few exceptional cases do these rates go above 0.6. In addition, the number of preconditioned GMRES(32) iterations is also fairly uniform for fixed N and varying values of β , the minimum eigenvalue of D , and different configurations. Further, although the number of preconditioned GMRES(32) iterations seems to grow slightly for the larger problem sizes, we see that the number of iterations is reduced by roughly two orders of magnitude when compared to the number of iterations needed by CGNR without preconditioning, as reported in Figure 3.2 for the odd-even system and in all tests the outer preconditioned GMRES(32) method never reaches a restart. Finally, we observe that in almost all cases the errors and residuals are within an order of magnitude, which further demonstrates the effectiveness of the proposed method.

4.2. The 2D Wilson matrix – Bootstrap super-V cycle setup . In this section, to test the impact of the coarsest-grid eigensolver on the overall effectiveness of the bootstrap AMG process, we consider a modified setup cycle in which the number of relaxations used on each grid is the same as in an overall W cycle, but each grid is visited only once. Specifically, we consider a $V(\mu 2^l, \mu 2^l)$ cycle in the setup phase and as before $W(4, 4)$ cycles in the solve phase. Here, l denotes the given grid and the notation $V(\mu 2^l, \mu 2^l)$ means that we use $\mu 2^l$ pre-smoothing iterations and $\mu 2^l$ post-smoothing iterations on grid $l = 1, \dots, L - 1$. Thus, the number of smoothing steps applied on each grid is the same as in a $W(\mu, \mu)$ cycle, but the coarsest-grid eigensolve is applied only once. We use the same settings for the setup cycles as we used in Section 4.1, i.e., $k_r = k_e = 8$, $\mu = 10$ in the first super-V cycle setup, and $\mu = 5$ in the second setup cycle. We test the method for $N = 128$ and $\beta = 6$ and use the same nine gauge field configurations we used in the previous section.

The results of these tests are reported in Figure 4.3. As we can see in the plots on the left and in the middle in the figure, the stand-alone solver and preconditioner with this setup strategy is less effective than the one coming from the W cycle setup. Further, we see in the plots on the right that for some of the most ill-conditioned cases, the residuals and errors again differ by several orders of magnitude. Together, these results demonstrate the effectiveness of the method when the coarsest-grid eigensolver is repeated within the bootstrap setup process, especially in the most ill-conditioned cases.

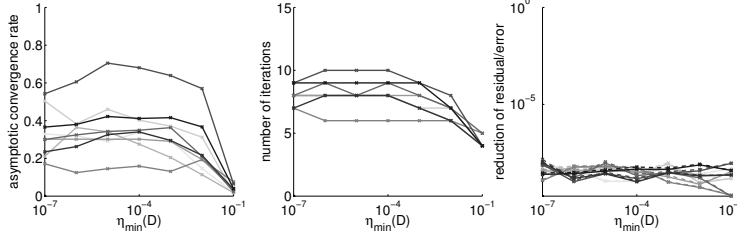
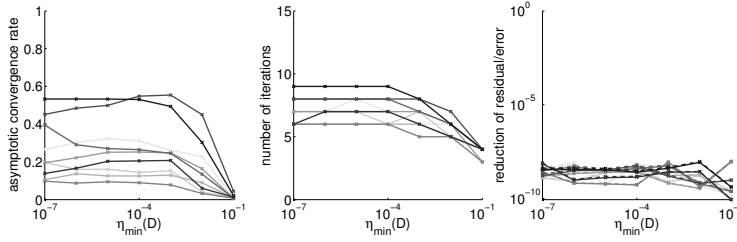
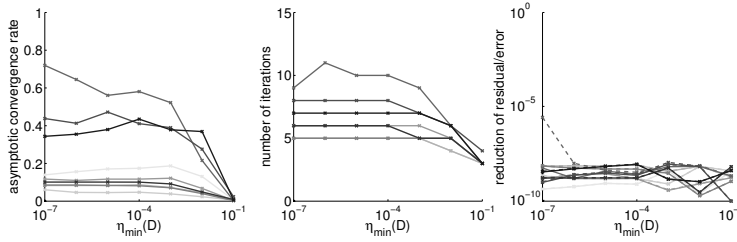

 (a) $N = 128$, $\beta = 3$

 (b) $N = 128$, $\beta = 6$

 (c) $N = 128$, $\beta = 10$

Fig. 4.1: Results of bootstrap AMG and bootstrap AMG preconditioned GMRES(32) applied to the odd-even reduced matrix for $N = 128$ and different values of β . The results for the light to dark lines correspond to different gauge field configurations, going from light to dark with increasing configuration number. On the left, plots of the estimates of the convergence rates ρ for the stand-alone solver versus $\eta_{\min}(D)$ defined in (2.4), corresponding to different diagonal shifts m , are provided. In the middle, the number of bootstrap AMG preconditioned GMRES(32) iterations needed to reduce the ℓ_2 norm of the relative residual by a factor of 10^{-8} is plotted against $\eta_{\min}(D)$. The plots on the right contain the ℓ_2 norms of the relative residuals (solid lines) and relative errors (dashed lines) computed using the resulting solution versus $\eta_{\min}(D)$.

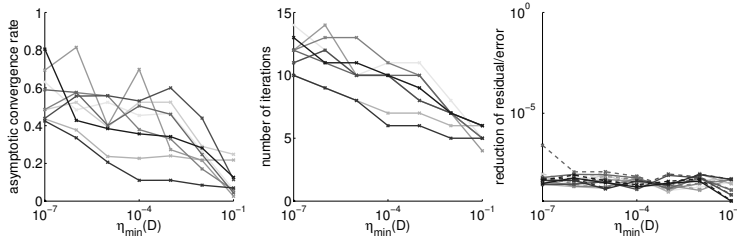
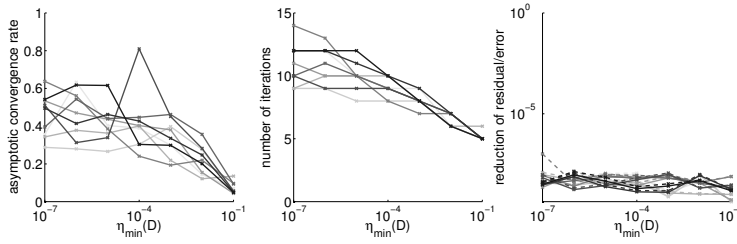
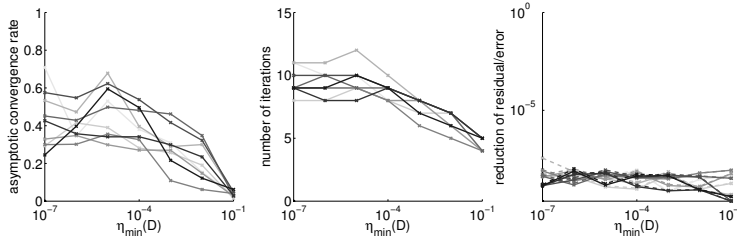
(a) $N = 256$, $\beta = 3$ (b) $N = 256$, $\beta = 6$ (c) $N = 256$, $\beta = 10$

Fig. 4.2: Results of bootstrap AMG and bootstrap AMG preconditioned GMRES(32) applied to the odd-even reduced matrix for $N = 256$ and different values of β . The results for the light to dark lines correspond to different gauge field configurations, going from light to dark with increasing configuration number. On the left, plots of the estimates of the convergence rates ρ for the stand-alone solver versus $\eta_{\min}(D)$ defined in (2.4), corresponding to different diagonal shifts m , are provided. In the middle, the number of bootstrap AMG preconditioned GMRES(32) iterations needed to reduce the ℓ_2 norm of the relative residual by a factor of 10^{-8} is plotted against $\eta_{\min}(D)$. The plots on the right contain the ℓ_2 norms of the relative residuals (solid lines) and relative errors (dashed lines) computed using the resulting solution versus $\eta_{\min}(D)$.

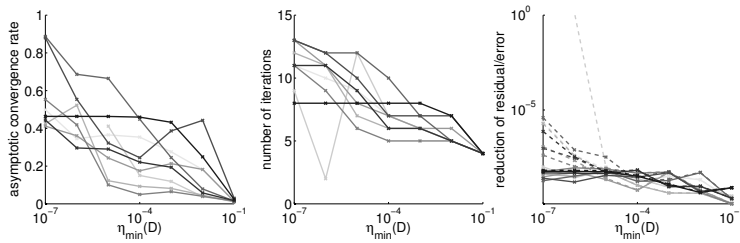


Fig. 4.3: Results of super-V cycle setup and W cycle bootstrap AMG and bootstrap AMG preconditioned GMRES(32) solvers applied to the odd-even reduced matrix for $N = 128$ and $\beta = 6$. The results for the light to dark lines correspond to different gauge field configurations, going from light to dark with increasing configuration number. On the left, plots of the estimates of the convergence rates ρ for the stand-alone solver versus $\eta_{\min}(D)$ defined in (2.4), corresponding to different diagonal shifts m , are provided. In the middle, the number of bootstrap AMG preconditioned GMRES(32) iterations needed to reduce the ℓ_2 norm of the relative residual by a factor of 10^{-8} is plotted against $\eta_{\min}(D)$. The plots on the right contain the ℓ_2 norms of the relative residuals (solid lines) and relative errors (dashed lines) computed using the resulting solution versus $\eta_{\min}(D)$.

5. Concluding Remarks. In this paper, we designed and tested a bootstrap approach for computing multigrid interpolation operators for the non-Hermitian Wilson discretization of the Dirac equation. As in any efficient multigrid solver, these operators have to be accurate for the near kernel vectors of the problem’s finest-grid operator. Here, this is achieved by defining interpolation to fit, in a least squares sense, a set of test vectors that collectively approximate the near-kernel vectors of the Dirac matrix. A main new result is given in Theorem 3.1, where we used the γ_5 -symmetry of the Wilson matrix to reduce a Petrov Galerkin multigrid algorithm for the non-Hermitian Wilson matrix D to a Galerkin approach for D , where the setup process is applied to the Hermitian and indefinite version $Z = \Gamma_5 D$ of the Wilson matrix to derive the solver for D (and Z).

Further, extensive numerical tests have shown that using least squares interpolation together with a bootstrap AMG setup based on an equivalent Hermitian indefinite form of the Wilson matrix and an intermediate adaptive setup cycle leads, in practice, to a robust AMG setup algorithm and thereby solver and preconditioner for the Wilson matrix over a wide range of problem parameters. All numerical experiments presented in the paper were carried out for Wilson’s discretization of the 2-dimensional Dirac equation on a structured grid, using full coarsening and interpolation with a fixed nearest neighbor sparsity pattern. This allowed us to concentrate on developing and testing least squares techniques for computing the interpolation operators and the impact of the bootstrap AMG setup, the multigrid eigensolver, and the adaptive step on the efficiency of the resulting multigrid solver. Generally, we have shown that with a proper choice of these components of the algorithm, a robust and efficient solver can be constructed. We note, in addition, that all of the derivations and heuristic arguments used in formulating the proposed algorithm carry over directly to the 4-dimensional Wilson matrix arising in Quantum Chromodynamic simulations so that

the proposed solver is expected to work well in this setting, too.

REFERENCES

- [1] R. Babich, J. Brannick, R. C. Brower, M. A. Clark, T. A. Manteuffel, S. F. McCormick, J. C. Osborn, and C. Rebbi. Adaptive multigrid algorithm for the lattice Wilson-Dirac operator. *Phys. Rev. Lett.*, 105:201602, Nov 2010.
- [2] Ronald Babich, James Brannick, Richard C. Brower, Michael A. Clark, Saul D. Cohen, et al. The Role of multigrid algorithms for LQCD. *PoS, LAT2009:031*, 2009.
- [3] R. Bank and T. Dupont. A comparison of two multilevel iterative methods for nonsymmetric and indefinite elliptic finite element equations. *SIAM J. Numer. Anal.*, 18:701–718, 1981.
- [4] M. Bolten, A. Brandt, J. Brannick, A. Frommer, K. Kahl, and I. Livshits. Bootstrap AMG for Markov chains. *SIAM J. Sci. Comput.*, 33:3425–3446, 2011.
- [5] J. Bramble, D. Y. Kwak, and J. Pasciak. Uniform convergence of multigrid V-cycle iterations for indefinite and nonsymmetric problems. In *Sixth Copper Mountain Conference on Multigrid Methods*, pages 43–59, 1993.
- [6] A. Brandt. Multiscale scientific computation: review 2001. In T. J. Barth, T. F. Chan, and R. Haimes, editors, *Multiscale and Multiresolution Methods: Theory and Applications*, pages 1–96. Springer, Heidelberg, 2001.
- [7] A. Brandt, J. Brannick, K. Kahl, and I. Livshits. Bootstrap AMG. *SIAM J. Sci. Comput.*, 33:612–632, 2011.
- [8] A. Brandt, S. McCormick, and J. Ruge. Algebraic multigrid (AMG) for automatic multigrid solution with application to geodetic computations. Technical report, Colorado State University, Fort Collins, Colorado, 1983.
- [9] A. Brandt, S. McCormick, and J. Ruge. Algebraic multigrid (AMG) for sparse matrix equations. In D. J. Evans, editor, *Sparsity and Its Applications*. Cambridge University Press, Cambridge, 1984.
- [10] J. Brannick and L. Zikatanov. Algebraic multigrid methods based on compatible relaxation and energy minimization. In O. B. Widlund and D. E. Keyes, editors, *Domain decomposition methods in science and engineering XVI*, volume 55, pages 15–26. Springer, 2007.
- [11] M. Brezina, R. Falgout, S. MacLachlan, T. Manteuffel, S. McCormick, and J. Ruge. Adaptive amg (aAMG). *SIAM J. Sci. Comput.*, 26:1261–1286, 2005.
- [12] M. Brezina, T. Manteuffel, S. McCormick, J. Ruge, and G. Sanders. Towards adaptive smooth aggregation (aSA) for nonsymmetric problems. *SIAM J. Sci. Comput.*, 32:4–39, 2010.
- [13] R. Brower, K. Moriarty, C. Rebbi, and E. Vicari. Variational multigrid for nonabelian gauge theory. In *Tallahassee 1990, Proceedings, Lattice 90* 89-93. (see HIGH ENERGY PHYSICS INDEX 29 (1991) No. 11041).
- [14] R. C. Brower, K. J. M. Moriarty, C. Rebbi, and E. Vicari. Multigrid propagators in the presence of disordered U(1) gauge fields. *Phys. Rev.*, D43:1974–1977, 1991.
- [15] Richard C. Brower, Robert G. Edwards, Claudio Rebbi, and Ettore Vicari. Projective multigrid for Wilson fermions. *Nucl. Phys.*, B366:689–705, 1991.
- [16] Richard C. Brower, Eric Myers, Claudio Rebbi, and K. J. M. Moriarty. The multigrid method for fermion calculations in Quantum Chromodynamics. Print-87-0335 (IAS, PRINCETON).
- [17] Richard C. Brower, Claudio Rebbi, and Ettore Vicari. Projective multigrid for propagators in lattice gauge theory. *Phys. Rev. Lett.*, 66:1263–1266, 1991.
- [18] Richard C. Brower, Claudio Rebbi, and Ettore Vicari. Projective multigrid method for propagators in lattice gauge theory. *Phys. Rev.*, D43:1965–1973, 1991.
- [19] T. DeGrand and C. E. Detar. *Lattice Methods for Quantum Chromodynamics*. World Scientific, 2006.
- [20] L. Del Debbio, Leonardo Giusti, M. Luscher, R. Petronzio, and N. Tantalo. Stability of lattice QCD simulations and the thermodynamic limit. *JHEP*, 0602:011, 2006.
- [21] A. Bazavov et. al. The MILC collaboration. *Rev. Mod. Phys.*, 82:1349–1417, 2010.
- [22] Andreas Frommer, Karsten Kahl, Stefan Krieg, Björn Leder, and Matthias Rottmann. Aggregation-based multilevel methods for lattice QCD. *pre-print*, arxiv:1202.2462v1, 2012. submitted.
- [23] C. Gattringer and C. B. Lang. Quantum Chromodynamics on the lattice. *Lect. Notes Phys.*, 788:1–211, 2010.
- [24] G. Golub and W. Kahan. Calculating the singular values and pseudo-inverse of a matrix. *Journal of the Society for Industrial and Applied Mathematics Series B Numerical Analysis*, 2(2):205–224, 1965.
- [25] M. Harmatz, P. G. Lauwers, R. Ben-Av, A. Brandt, E. Katznelson, S. Solomon, and

- K. Wolowesky. Parallel-transported multigrid and its application to the schwinger model. *Nuclear Physics B - Proceedings Supplements*, 20(0):102 – 109, 1991.
- [26] Tamas G. Kovacs, Ferenc Pittler, Falk Bruckmann, and Sebastian Schierenberg. High temperature quark localization by Polyakov loops. *PoS, LATTICE2011:200*, 2011.
 - [27] C. Lanczos. *Linear Differential Operators*. van Nostrand, 1961.
 - [28] R. Falgout M. Brezina, S. MacLachlan, T. Manteuffel, S. McCormick, and J. Ruge. Adaptive smoothed aggregation (α SA). *SIAM J. Sci. Comput.*, 25(6):1896–1920, 2004.
 - [29] I. Montvay and G. Münster. *Quantum Fields on a Lattice*. Cambridge Monographs on Mathematical Physics Series. Cambridge University Press, 1994.
 - [30] J. C. Osborn, R. Babich, J. Brannick, R. C. Brower, M. A. Clark, et al. Multigrid solver for clover fermions. *PoS, LATTICE2010:037*, 2010.
 - [31] Constantin Popa. Algebraic multigrid smoothing property of Kaczmarz’s relaxation for general rectangular linear systems. *Electron. Trans. Numer. Anal.*, 29:150–162, electronic only, 2007.
 - [32] Marzio Sala and Raymond S. Tuminaro. A new Petrov-Galerkin smoothed aggregation preconditioner for nonsymmetric linear systems. *SIAM J. Sci. Comput.*, 31(1):143–166, October 2008.
 - [33] H. Sterck. A self-learning algebraic multigrid method for extremal singular triplets and eigenpairs. *SIAM J. Sci. Comput.*, 34(4):A2092–A2117, 2012.
 - [34] Ulrich Trottenberg and Anton Schuller. *Multigrid*. Academic Press, Inc., Orlando, FL, USA, 2001.
 - [35] P. Vassilevski. *Multilevel Block Factorization Preconditioners: Matrix-based Analysis and Algorithms for Solving Finite Element Equations*. Springer, 2009.
 - [36] Kenneth G. Wilson. Confinement of quarks. *Phys. Rev. D*, 10:2445–2459, Oct 1974.